The Effect of Magnetic Field Geometry on Viscous Damping of Rotation in Stellarators

H. Wobig, J. Kißlinger

IPP 2/334 January 1997

MAX-PLANCK-INSTITUT FÜR PLASMAPHYSIK

85748 GARCHING BEI MÜNCHEN

MAX-PLANCK-INSTITUT FÜR PLASMAPHYSIK

GARCHING BEI MÜNCHEN

The Effect of Magnetic Field Geometry on Viscous Damping of Rotation in Stellarators

H. Wobig, J. Kißlinger

IPP 2/334 **January 1997**

Max-Planck-Institut für Plasmaphysik, EURATOM-Association, Garching bei München

Die nachstehende Arbeit wurde im Rahmen des Vertrages zwischen dem Max-Planck-Institut für Plasmaphysik und der Europäischen Atomgemeinschaft über die Zusammenarbeit auf dem Gebiete der Plasmaphysik durchgeführt.

I. Introduction.

Poloidal rotation with shear flow is one of the key elements in the theory of H-mode confinement in toroidal systems. There are various driving forces which may excite poloidal and toroidal rotation, Stringer spin-up, turbulent Reynolds stresses and lost orbits. Viscous damping is the main candidate to retard the rotation. In a collision dominated plasma viscous damping is provided by the magnetic pumping effect which arises from the variation of the magnetic field strength along the stream lines of rotation. It only depends on the Fourier spectrum of B on magnetic surfaces and not on the details of particle orbits. A comparison of viscous damping rates of various toroidal configurations has been given in [1]. In the plateau regime the poloidal viscous damping rate has been calculated by K.C Shaing[2] and J.N.Talmadge et al.[3]. In these papers the interest is focussed on the dependence on the electric field which reduces the damping rate at large fields and thus may give rise to multiple solutions. The non-axisymmetric components in the Fourier spectrum of B lead to extra maxima in the poloidal force which complicates the bifurcation problem as compared to axisymmetric tokamaks. Enhanced poloidal damping also occurs if magnetic islands exist in the confinement region. In stellarators islands occur on rational magnetic surfaces if there exists a resonant field perturbation. Such perturbations always exist on "natural surfaces" with the rotational transform

$$\iota = M/k \quad ; \; k = 1,2,3,4,...$$

M is the number of field periods . The denominator indicates the number of islands. Symmetry breaking field perturbations introduce another class of islands which can easily dominate over the natural islands. In general there is a combination of natural islands and symmetry breaking islands. Examples are given by the Wendelstein stellarators W 7-A and W 7-AS[4]. Islands lead to enhanced radial transport and therefore also to enhanced poloidal damping. In the neighbourhood of islands magnetic surfaces are modified and the Fourier spectrum of B exhibits harmonics with the periodicity of the island. Due to toroidal curvature the field variation on magnetic surfaces is roughly

$$\delta B/B = r/R \tag{1}$$

r is the average radius of the magnetic surface and R the major radius. This component is the contribution to the poloidal viscous damping rate. If the island has a half width δr , the field variation on magnetic surfaces close to the separatrix of the island is

$$\left(\delta B/B\right)_{m,l} \approx \delta r/R \sin\left(m\varphi - l\theta\right) \tag{2}$$

θ is the poloidal angle and φ the toroidal angle.

---

[1] J. Kisslinger, H. Wobig , " On rotation of collisional plasmas in toroidal systems ", Plasma Phys. Contr. Fusion **37** (1995) 893 - 922

[2] K.C. Shaing, Phys. Fluids 5 No. 11 (1993) , 3841-3843

[3] J.N. Talmadge, B.J. Peterson,D.T. Anderson, F.S.B. Anderson, H. Dahl, J.L. Shohet, M. Coronado, K.C. Shaing,
15th IAEA-Conf. on PLasma Phys. and Contr. Nucl. Fus. Seville 1994, paper CN-60/A-6-I-6

[4] R. Jaenicke, K. Schwoerer, E. Ascasibar, P. Grigull, I. Lakicevic, M. Zippe, Proc. of 16th EPS-Conf. on Contr. Fus. and Plasma Phys. Venice 1989, Pt II, 627

In the following it will be shown how these islands modify the viscous damping rates in stellarators. In the collisional regime the effect is small, the viscous damping rate in the vicinity of islands can increase by factor of 2, however, in the plateau regime, where barely trapped particles dominate neoclassical transport resonances will occur which enhance the damping rates appreciably. The orbits of barely trapped particles are strongly modified by magnetic islands and thus lead to enhanced neoclassical transport and viscous damping. Even if no islands are present in the plasma region magnetic surfaces at the plasma edge are modified by resonant Fourier harmonics. This in particular occurs in the boundary region of Wendelstein 7-AS, where the last magnetic surfaces exhibit the M/k structure of the natural islands.

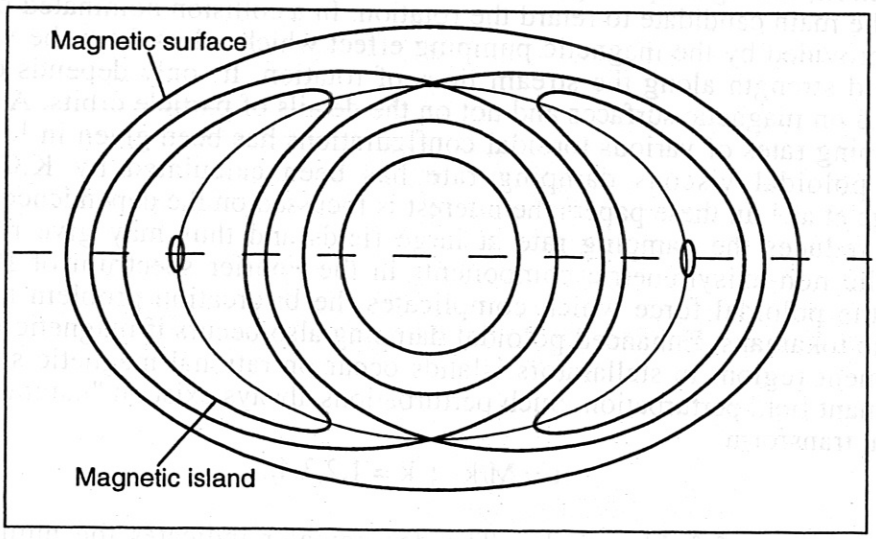

Fig. 1: Scheme of magnetic surfaces modified by magnetic islands.

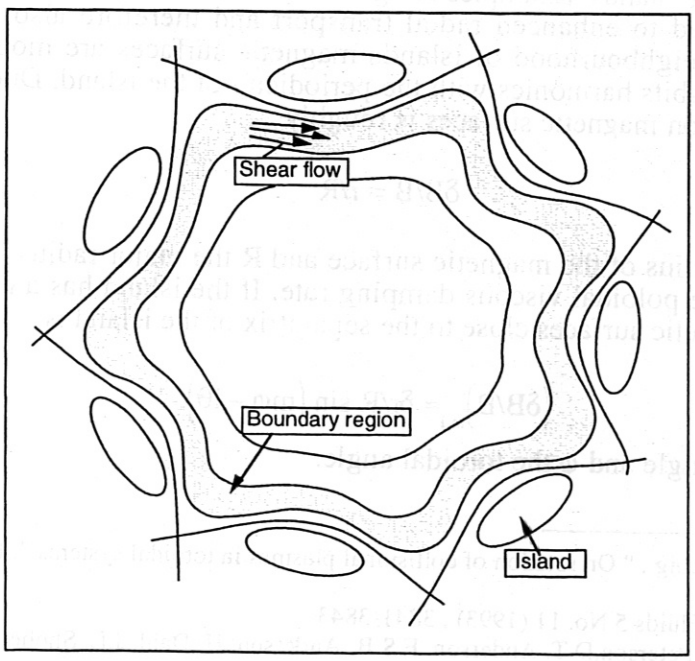

Fig. 2: Boundary region of a stellarator with natural islands

II Plasma Equilibrium

In the following we start from a magnetic field configuration with nested magnetic surfaces which satisfies the condition of ideal equilibrium

$$\mathbf{j} \times \mathbf{B} = \nabla p \tag{3}$$

On the magnetic surfaces the Hamada coordinate system is introduced which is characterised by straight magnetic field and a Jacobian equal to unity. In this coordinate system (s,θ,φ) the base vectors are defined by

$$\mathbf{e}_p = \nabla s \times \nabla \varphi \quad ; \quad \mathbf{e}_t = -\nabla s \times \nabla \theta \tag{4}$$

$\mathbf{e}_p$ is the poloidal base vector and $\mathbf{e}_t$ the toroidal base vector. s is the volume of the magnetic surface. The Jacobian is

$$\left(\nabla s \times \nabla \varphi\right) \cdot \nabla \theta = 1 \quad .$$

The dimension of the base vectors is a length. The rotational transform is defined by

$$\iota = \frac{\mathbf{B} \bullet \nabla \theta}{\mathbf{B} \bullet \nabla \varphi} = \frac{\chi'(s)}{\psi'(s)} \tag{5}$$

The magnetic field can be represented by

$$\mathbf{B} = \psi'(s)\mathbf{e}_t + \chi'(s)\mathbf{e}_p \tag{6}$$

and the plasma current

$$\mathbf{j} = I'(s)\mathbf{e}_t + J'(s)\mathbf{e}_p \tag{7}$$

The plasma current can also be written in the forrm

$$\mathbf{j} = -p'(\psi)\mathbf{e}_p + I'(\psi)\mathbf{B} \tag{8}$$

where instead of the volume s the toroidal flux ψ has been introduced as a label of the flux surfaces. Onto this equilibrium an arbitrary rotation in poloidal and toroidal direction can be superimposed. Since in ideal equilibrium there is no coupling between rotation and momentum balance this rotation is underdetermined as long as dissipative terms and inertial forces are neglected. This lowest order rotation stays on magnetic surfaces and satisfies the equations

$$-\nabla \Phi_o + \mathbf{v}_o \times \mathbf{B} = 0 \quad ; \quad \nabla \cdot \rho \mathbf{v}_o = 0 \tag{9}$$

which leads to the ansatz

$$\mathbf{v}_o = -E(\psi)\mathbf{e}_p + \Lambda(\psi)\mathbf{B} \; . \tag{10}$$

The two flux functions E and Λ describe the poloidal and the parallel motion on magnetic surfaces. E is the radial electric field. Because of the helical structure of the magnetic field the

parallel flow also contributes to the poloidal flow. In terms of the poloidal and toroidal base vectors the velocity is

$$\mathbf{v}_o = \left(-E(\psi) + \chi'(s)\Lambda(\psi) \right)\mathbf{e}_p + \Lambda(\psi)\psi'(s)\mathbf{e}_t \tag{11}$$

The poloidal flow consists of two parts, the electric drift and the poloidal component of the parallel flow. In next order these quantities must be computed from the balance between spin-up forces and dissipative forces (friction and viscosity). The spin-up is provided either by turbulent Reynolds stresses or by the Stringer mechanism.

III Viscous Forces

The viscous forces (or the magnetic pumping effect) are proportional to the lowest order velocities. These surface-averaged viscous forces are

$$\begin{pmatrix} -<\mathbf{e}_p \bullet \nabla \bullet \pi> \\ <\mathbf{B} \bullet \nabla \bullet \pi> \end{pmatrix} = \begin{pmatrix} \mu_p & \mu_b \\ \mu_b & \mu_t \end{pmatrix} \begin{pmatrix} E \\ \Lambda \end{pmatrix} \tag{12}$$

The viscous tensor π is defined by

$$\pi = m \int (\mathbf{v}:\mathbf{v} - \frac{v^2}{3}) f(\mathbf{v})\, d^3\mathbf{v} \tag{13}$$

or in Chew-Goldberger Low approximation

$$\begin{aligned} <\mathbf{e}_p \bullet \nabla \bullet \pi> &= <\left(p_{\parallel} - p_{\perp}\right)\mathbf{e}_p \bullet \frac{\nabla B}{B}> \\ <\mathbf{B} \bullet \nabla \bullet \pi> &= <\left(p_{\parallel} - p_{\perp}\right)\mathbf{B} \bullet \frac{\nabla B}{B}> \end{aligned} \tag{14}$$

In a collision-dominated plasma a general form of the anisotropic part of the pressure can be given

$$\left(p_{\parallel} - p_{\perp}\right) = -3\tau P \frac{\mathbf{B}}{B^2} \bullet \mathbf{B}\, \nabla\, \mathbf{v}_o \tag{15}$$

$P = nkT$ is the scalar pressure and τ is the ion-ion collision time. This equation describes the magnetic pumping effect. Inserting eq. 15 into eq. 14 leads to the viscous forces in the following form

$$\begin{pmatrix} -<\mathbf{e}_p \bullet \nabla \bullet \pi> \\ <\mathbf{B} \bullet \nabla \bullet \pi> \end{pmatrix} = 3\tau P \begin{pmatrix} C_p & C_b \\ C_b & C_t \end{pmatrix} \begin{pmatrix} E \\ \Lambda \end{pmatrix} \tag{16}$$

The geometric coefficients C are given by

$$C_p = <\left(\mathbf{e}_p \bullet \frac{\nabla B}{B}\right)^2> \;;\; C_t = <\left(\mathbf{B} \bullet \frac{\nabla B}{B}\right)^2> \;;\; C_b = <\left(\mathbf{e}_p \bullet \frac{\nabla B}{B}\right)\left(\mathbf{B} \bullet \frac{\nabla B}{B}\right)> \tag{17}$$

C_p couples the toroidal velocity to the poloidal force and C_t the toroidal velocity to the toroidal viscous force. The cross coupling is described by C_b. Expanding the magnetic field in a Fourier series

$$\ln B = \sum_{l,m}^{\infty} b_{lm} \exp\left(il\theta + im\varphi\right)$$

yields the coefficients as a series

$$C_p = \sum_{l,m}^{\infty} |b|_{lm}^2 l^2$$

$$C_t = \sum_{l,m}^{\infty} |b|_{lm}^2 \left(\chi' l + \psi' m\right)^2$$

$$C_b = \sum_{l,m}^{\infty} |b|_{lm}^2 \chi' \psi' lm \qquad (18)$$

Magnetic islands distort the magnetic surfaces in its vicinity as discussed above. The Fourier spectrum will be modified and especially Fourier harmonics with

$$\chi' l + \psi' m = 0$$

or the neighbouring side bands will be increased. This will have only little effect on the parallel coefficient C_t, however the other two coefficients C_p and C_b will be enhanced. The mixed coefficient C_b is the relevant coefficient of the classical bootstrap effect, the correlation between this coefficient and the toroidal current is discussed in [5]. In stellarators without sysmmetries - neither axisymmetry nor helical symmetry - there is a finite threshold for spin-up which is given by

$$R_{11} = 3\tau P \left(\frac{C_b^2}{C_t} - C_p\right) \qquad (19)$$

The term in brackets is purely geometrical and can be evaluated for any magnetic field. In an axisymmetric tokamak this threshold does not exist. To prove this statement we use the representation of the magnetic field given in eq. (6) and note that the toroidal variation of the magnetic field is zero.

$$\mathbf{B} \bullet \frac{\nabla B}{B} = \chi'(s) \mathbf{e}_p \bullet \frac{\nabla B}{B} \qquad (20)$$

Therefore the following relations among the viscous coefficients exist

$$C_b = < \left(\mathbf{e}_p \bullet \frac{\nabla B}{B}\right) \left(\mathbf{B} \bullet \frac{\nabla B}{B}\right) > = \chi'(s) C_p \qquad (21)$$

$$C_t = < \left(\mathbf{B} \bullet \frac{\nabla B}{B}\right)^2 > = \left(\chi'(s)\right)^2 C_p \qquad (22)$$

In this case the determinant in eq. 19 is zero. The same statement holds for helically invariant

---

[5] H. Wobig, On rotation of multispecies plasmas in toroidal systems, Plasma Phys. Contr. Fusion 38, (1996), 1053

configurations.

The following figure shows a comparison of this geometrical factor between Wendelstein 7-AS and Wendelstein 7-X. Wendelstein 7-B is an l=2 stellarator configuration with aspect ratio 10.

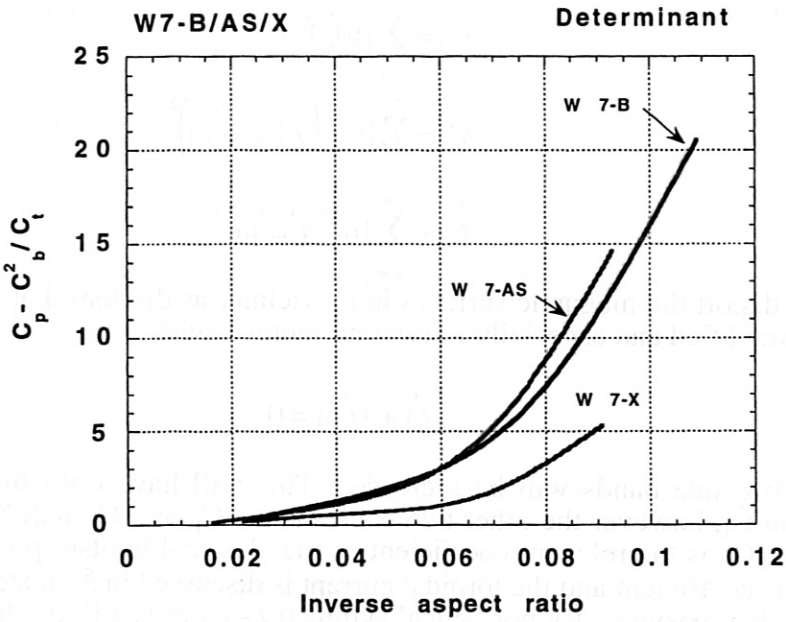

Fig. 3: Threshold of rotational spin-up defined by viscous forces (collisional regime).

These coefficients increase towards the plasma boundary. However, since these coefficients are multiplied by τP which decreases strongly towards the boundary the viscous forces are small in the boundary region. This may explain why plasma rotation is mainly observed in the boundary regions. The difference of the geometrical coefficients between Wendelstein 7-X and Wendelstein 7-AS suggests that plasma rotation in W 7-X could be more easily achieved than in W 7-AS. Further details of these computations are given in [6].

[6] J. Kisslinger, H. Wobig , " On rotation of collisional plasmas in toroidal systems ", Plasma Phys. Contr. Fusion **37** (1995) 893 - 922

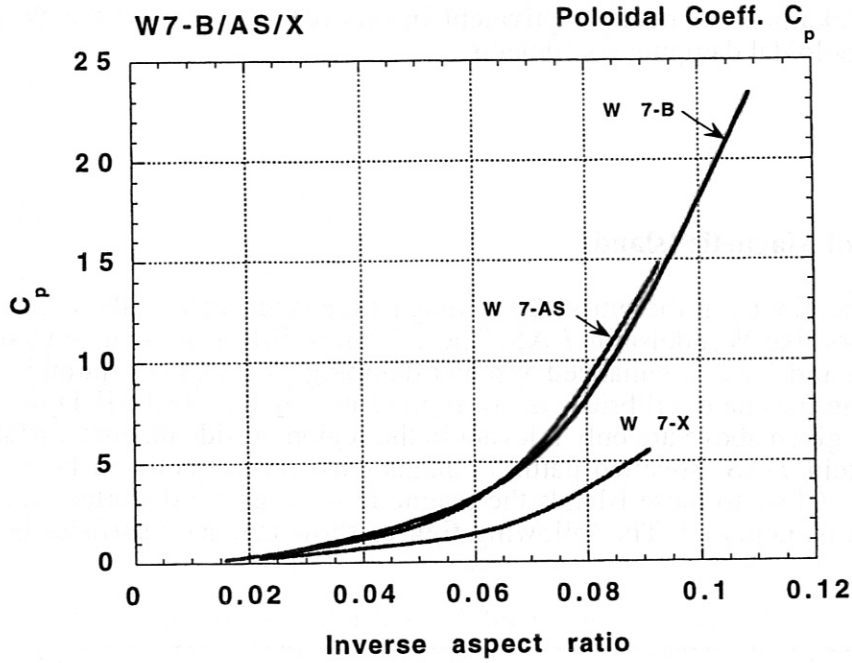

Fig. 4: Poloidal viscous coefficient C_p of various stellarators.

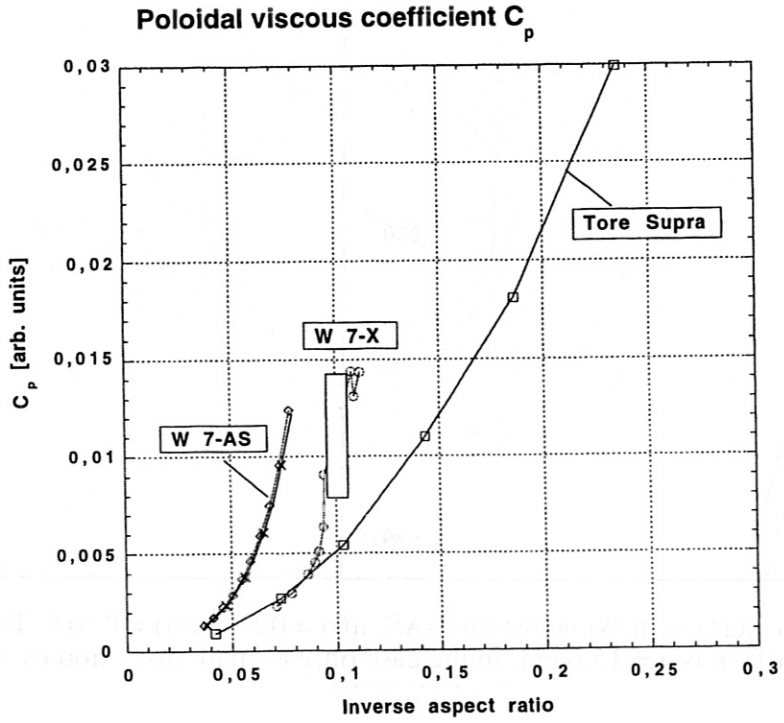

Fig. 5: Comparison with tokamak. Poloidal viscous coefficient. The gray rectangular region is the island at the boundary of W 7-X. The 2 curves of W 7-AS differ by the rotational transform.

In axisymmetric configurations like tokamaks a viscous damping in toroidal direction does not exist. The poloidal variation of B is determined by the 1/R-dependence. Fig. 5 shows the poloidal viscous coefficient of a circular tokamak in comparison with advanced stellarators. W 7-X and a tokamak are nearly equivalent in this respect whereas the W 7-AS device exhibits larger poloidal damping coefficients.

IV The Effect of Magnetic Islands

As already mentioned in the introduction magnetic islands arise in the boundary region of some stellarators like Wendelstein 7-AS. These islands distort the magnetic surfaces in the neighbourhood and lead to enhanced viscous damping (or magnetic pumping). Inside the island region the plasma equilibrium is not represented by the ideal MHD-theory, therefore the coefficients given above are only relevant in the region outside magnetic islands.

In Wendelstein 7-AS socalled natural islands exist on magnetic surfaces with $\iota = 5/n$; n=8,9,10,11 ,... Close to these islands the magnetic surfaces are distorted and the magnetic pumping effect is increased. The following figures show magnetic surfaces between $\iota = 0.5$ and $\iota = 0.556$.

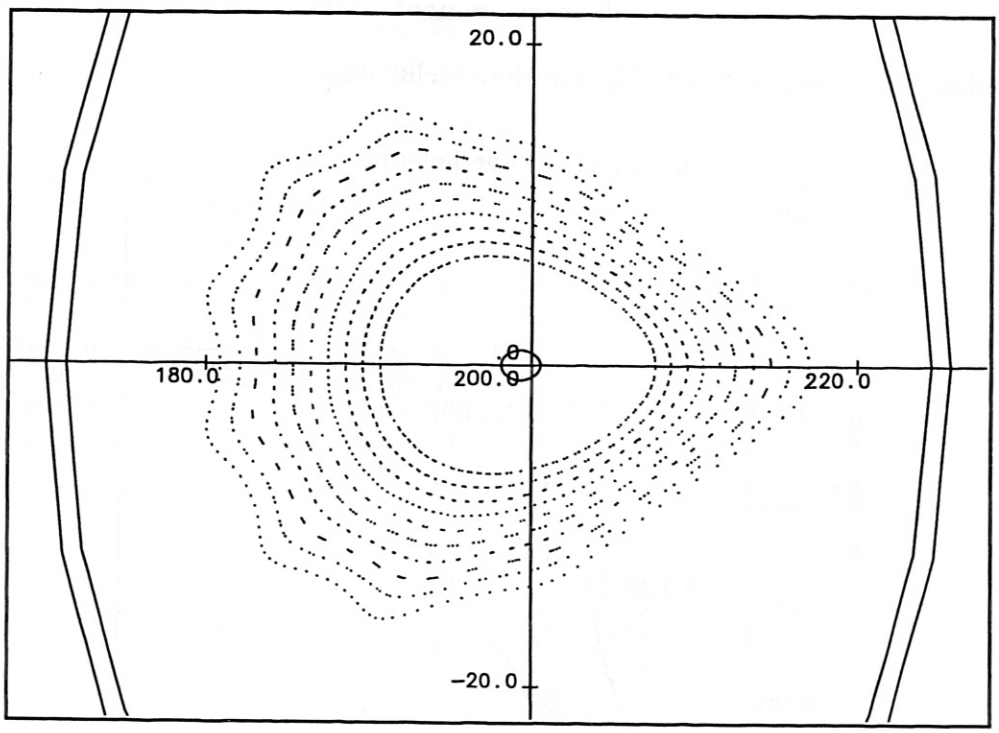

Fig. 6: Magnetic surface in Wendelstein 7-AS. $\iota(0) = 0.505$, $\iota(a) = 0.518$. The radius of the last magnetic surface is a = 15.6 cm. In the case only a small distortion by external islands occurs.

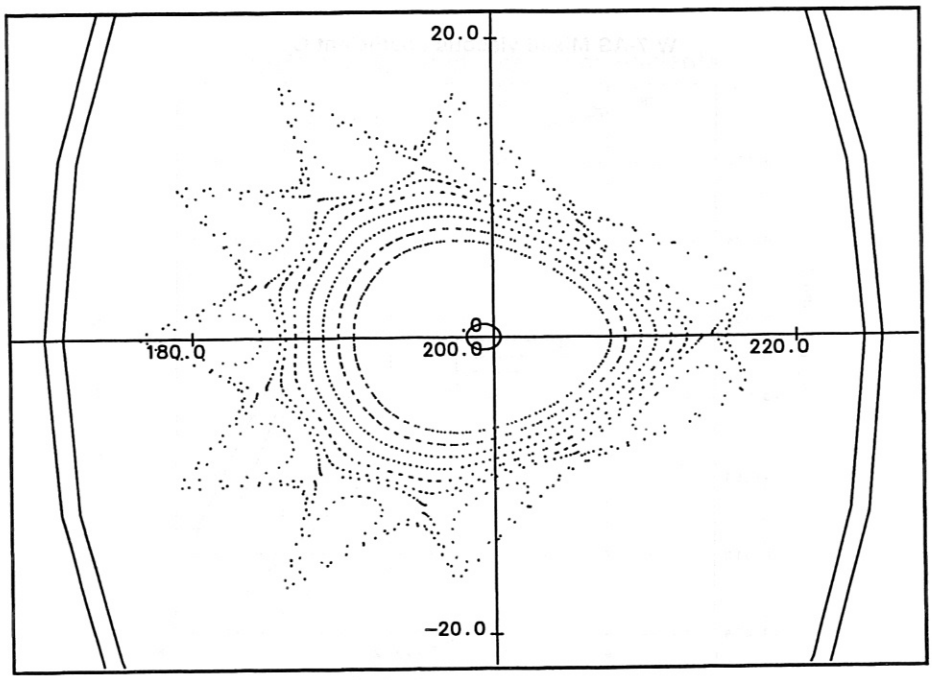

Fig. 7: W 7-AS. Magnetic surface with islands in the boundary region. $\iota(0) = 0.53$, $\iota(a) = 0.556$.The distortion of the Fourierspectrum of $B(\varphi,\theta)$ in the vicinity of the islands leads to an increase of the poloidal viscous coefficient as shown in the following figure.

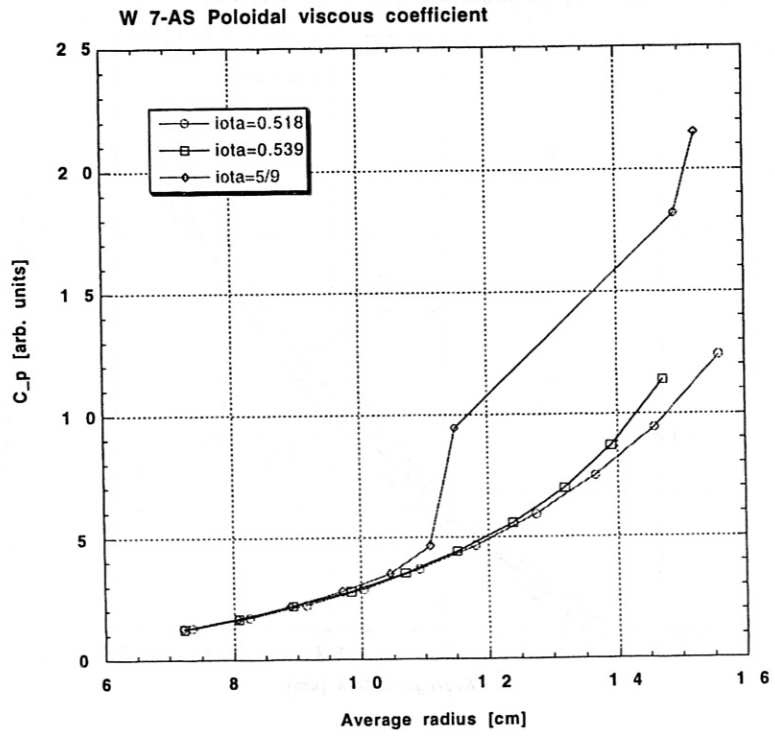

Fig. 8: Poloidal viscous damping rate C_p (collisional regime) in Wendelstein 7-AS. The regime of the rotational transform is between 5/10 and 5/9. The absissa is the average radius of the magnetic surface. Close to the island the damping rate is enhanced by a factor of 2. The coefficient C_b exhibits a similar enhancement as can be seen on the next figure.

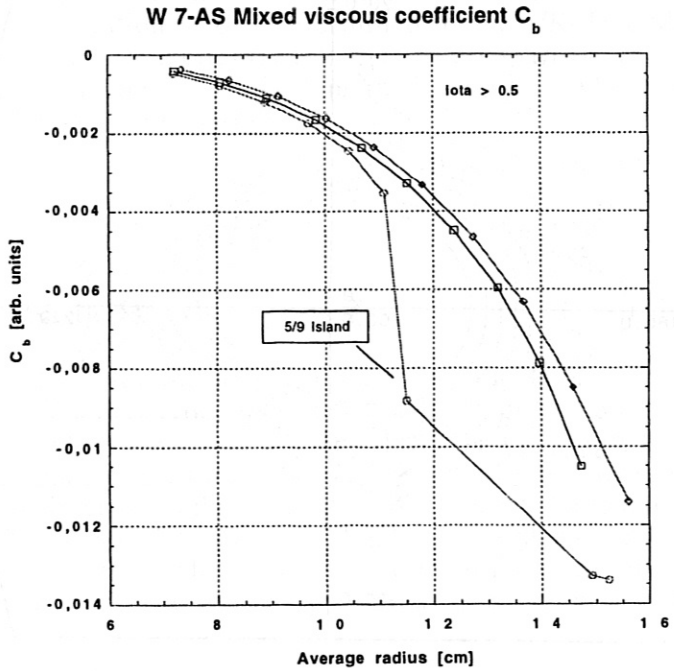

Fig. 9: W 7-AS. Viscous coefficient C_b vs average radius.

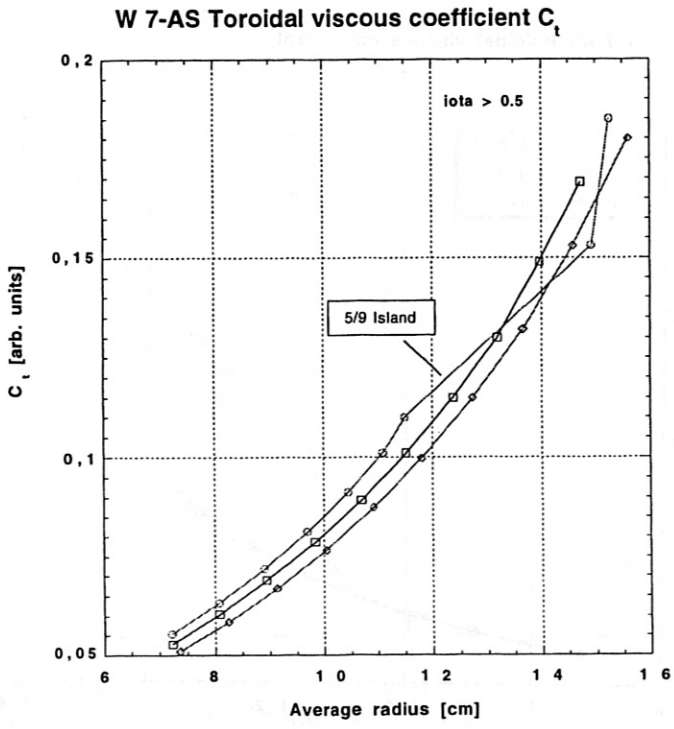

Fig. 10: W 7-AS. Parallel viscous coefficient C_t in the regime $\iota > 0.5$.

Little effect is seen on the parallel coefficient C_t.The threshold for poloidal spin-up is determined by the determinant $C_p - C_b * C_b / C_t$, which shows a similar behaviour as C_p.

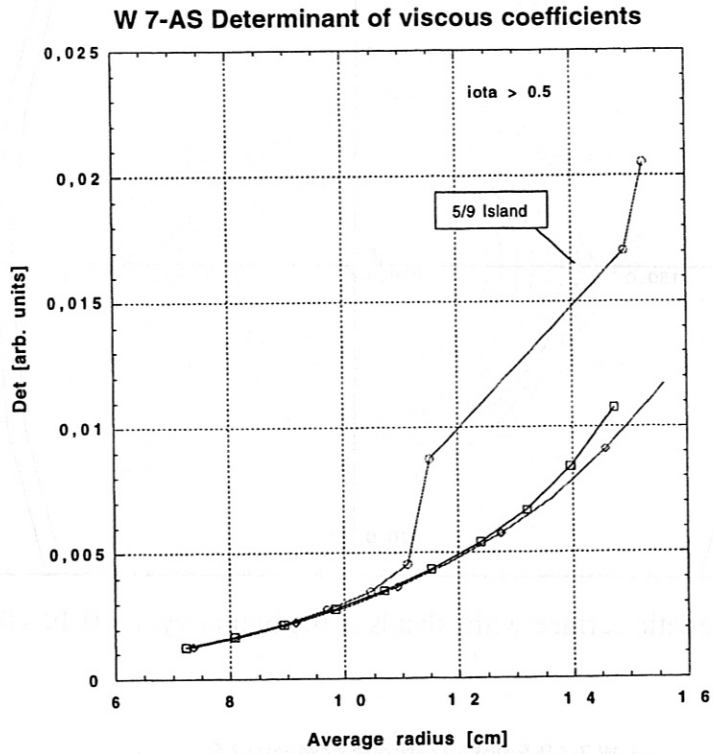

Fig. 11: W 7-AS. Determinant $D= C_p - C_b * C_b / C_t$ in the regime $\iota > 0.5$. In the regime below $\iota = 0.5$ a similar situation exists, the following figures show magnetic surfaces in this regime.

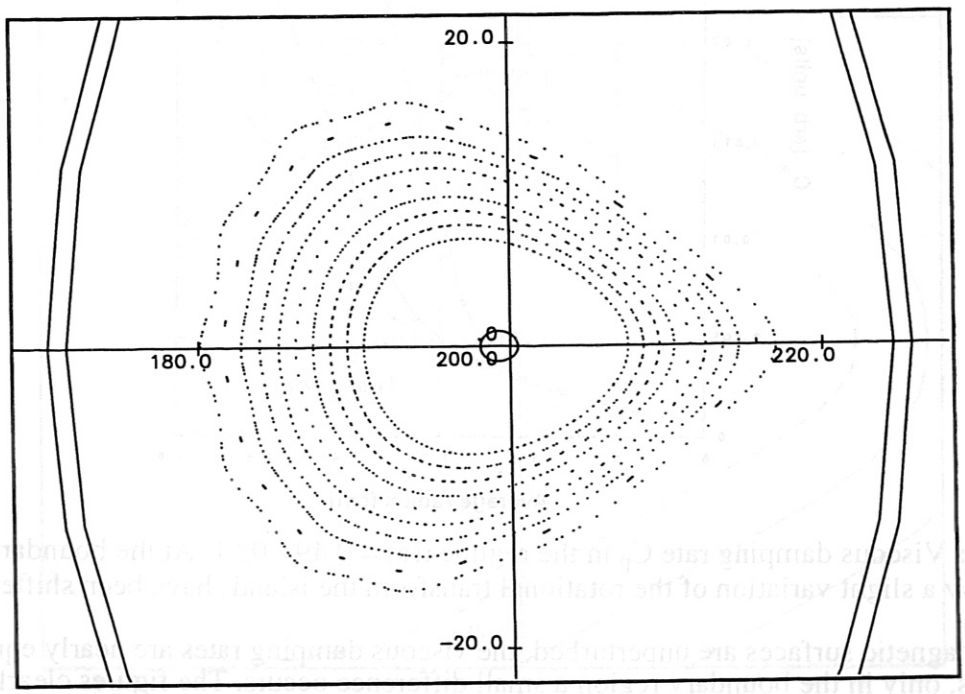

Fig. 12: W 7-AS. Nearly unperturbed magnetic surface in the regime $\iota = 0.47 - 0.48$

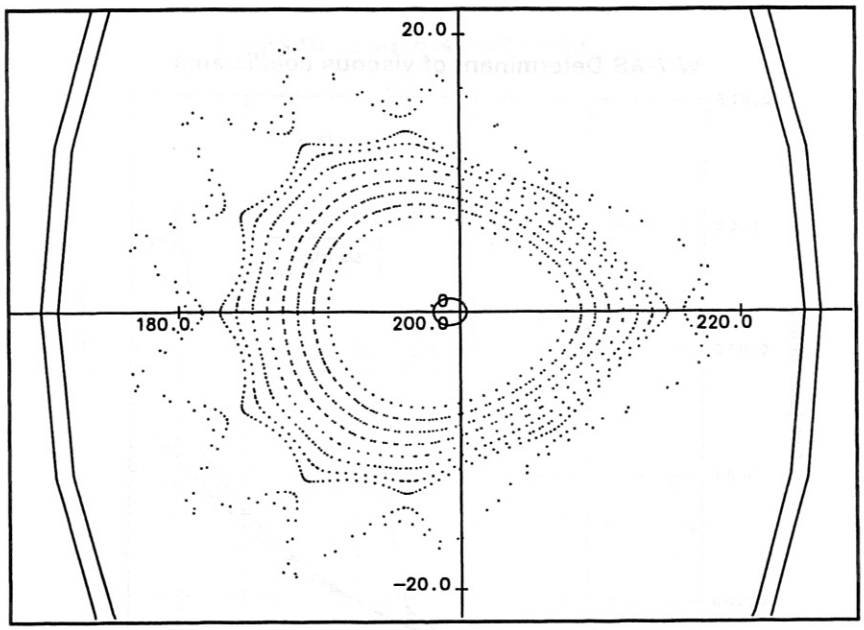

Fig. 13: W 7-AS. Magnetic surface with islands at the boundary. $\iota = 0.49 - 0.5$.

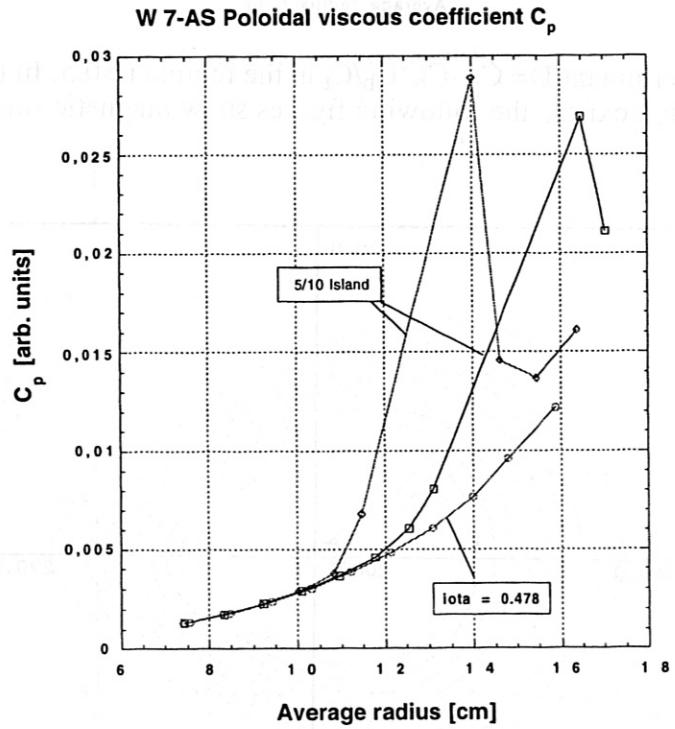

Fig. 14: Viscous damping rate C_p in the regime $\iota(a) = 0.49 - 0.51$. At the boundary 10 islands exist. By a slight variation of the rotational transform the islands have been shifted inwards.

If the magnetic surfaces are unperturbed, the viscous damping rates are nearly equal in these regimes, only in the boundary region a small difference occurs. The figures clearly show that viscous damping is increased in the neighbourhood of islands, therefore plasma rotation is impeded by these islands.

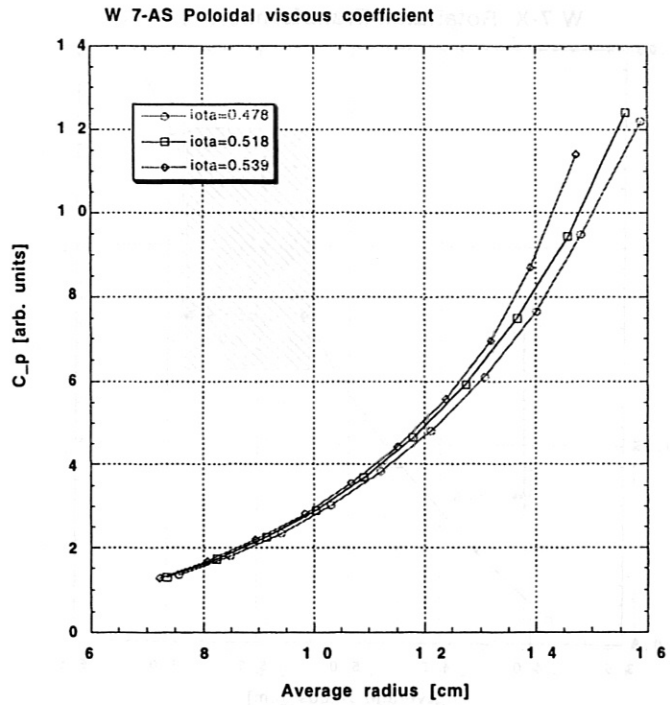

Fig. 15 : Wendelstein 7-AS. Viscous damping rate C_p on unperturbed surfaces.

In Wendelstein 7-X the standard case has 5 islands at the boundary. These islands are the base of the divertor concept and the issue arises whether these islands suppress plasma rotation in this region. The magnetic surface of the standard case is given in the following figure.

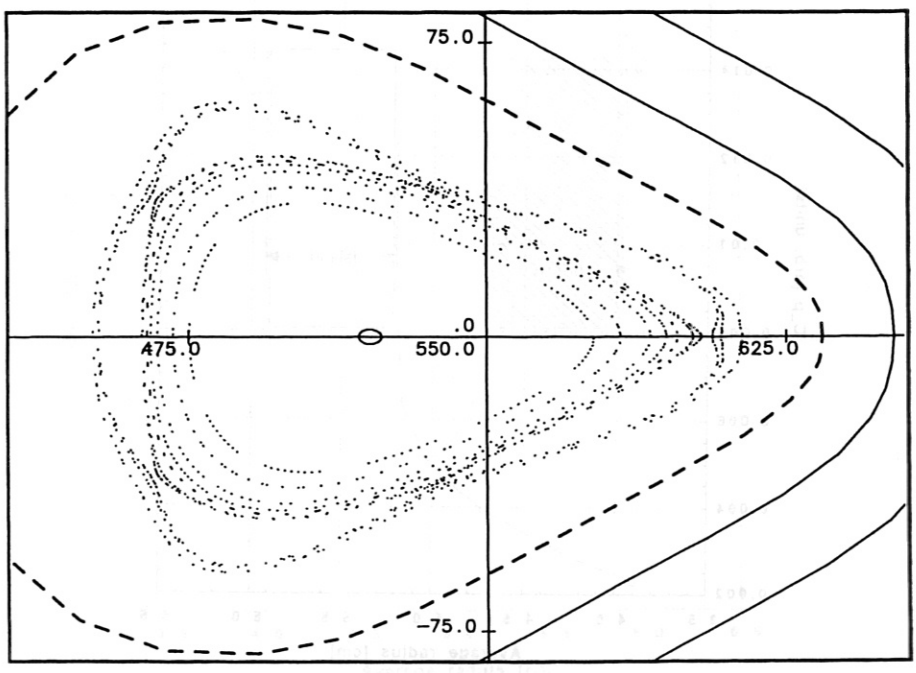

Fig. 16: Magnetic surfaces in Wendelstein 7-X.

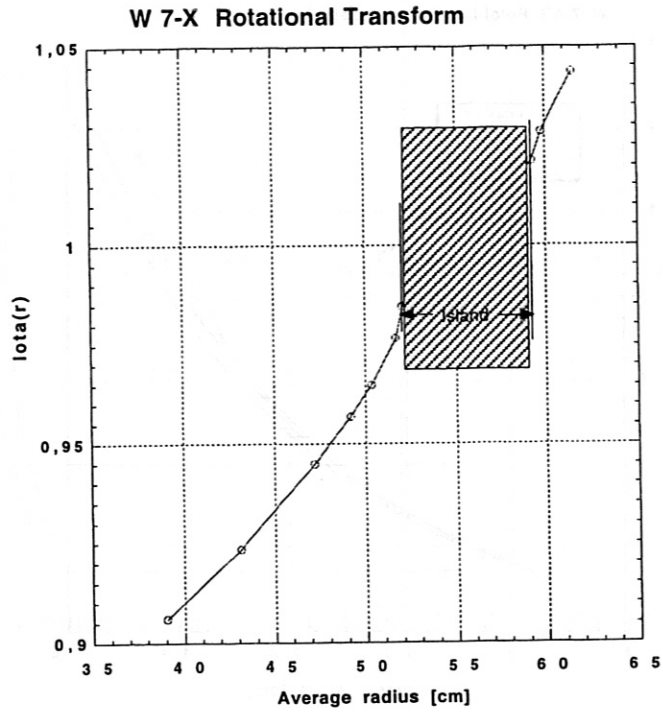

Fig. 17: Rotational transform vs average radius in Wendelstein 7-X

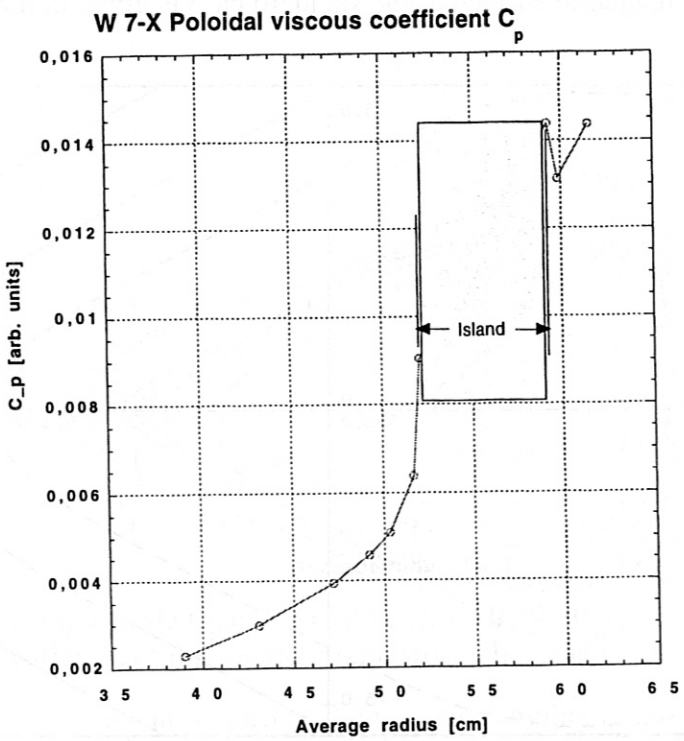

Fig. 18: Poloidal viscous coefficient C_p in Wendelstein 7-X

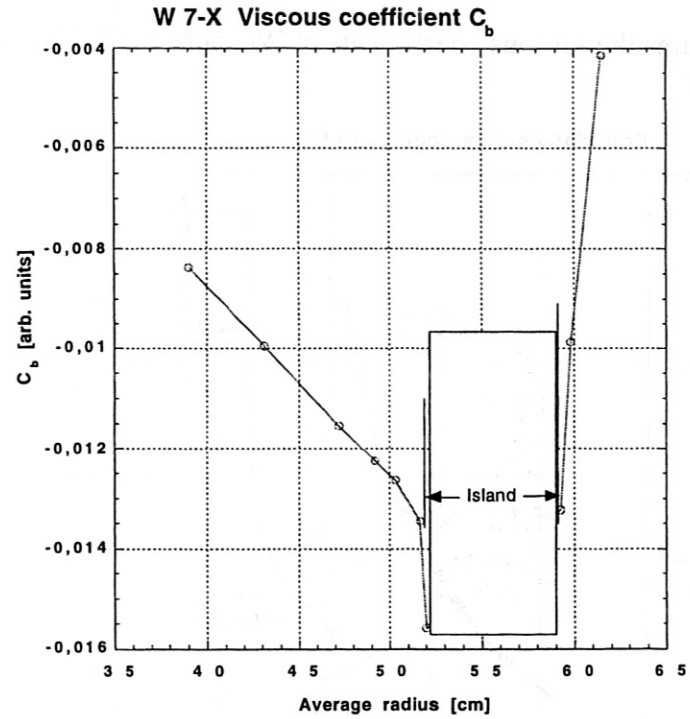

Fig. 19: Mixed viscous coefficient C_b in Wendelstein 7-X

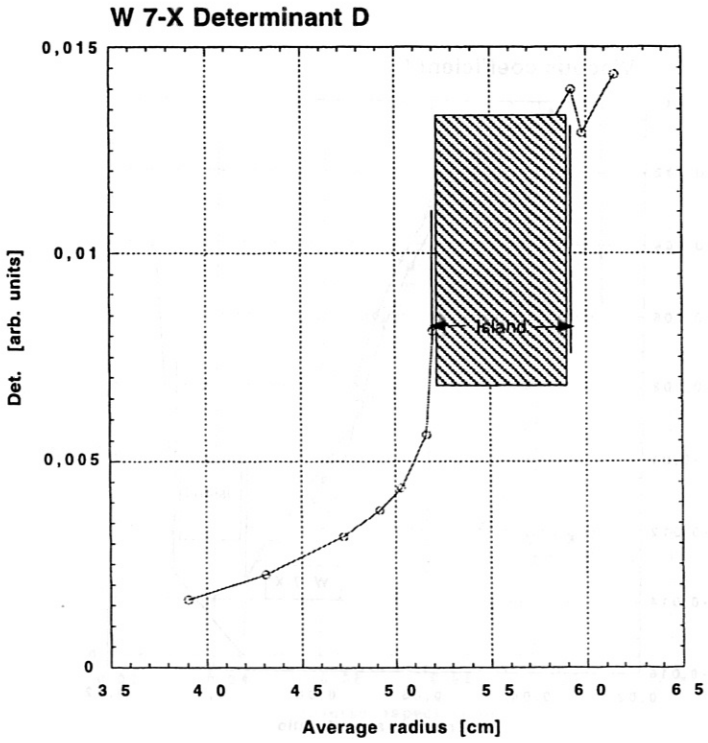

Fig. 20: Determinant (threshold) in Wendelstein 7-X

V Comparison with Wendelstein 7-AS.

In the next series of figures the viscous coefficients of Wendelstein 7-AS and Wendelstein 7-X are plotted together.

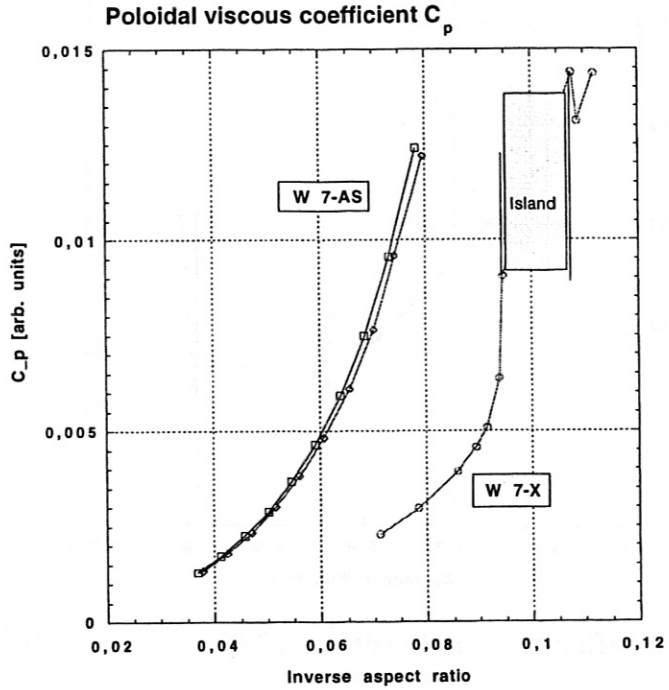

Fig. 21: Poloidal coefficients in Wendelstein 7-AS and 7-X

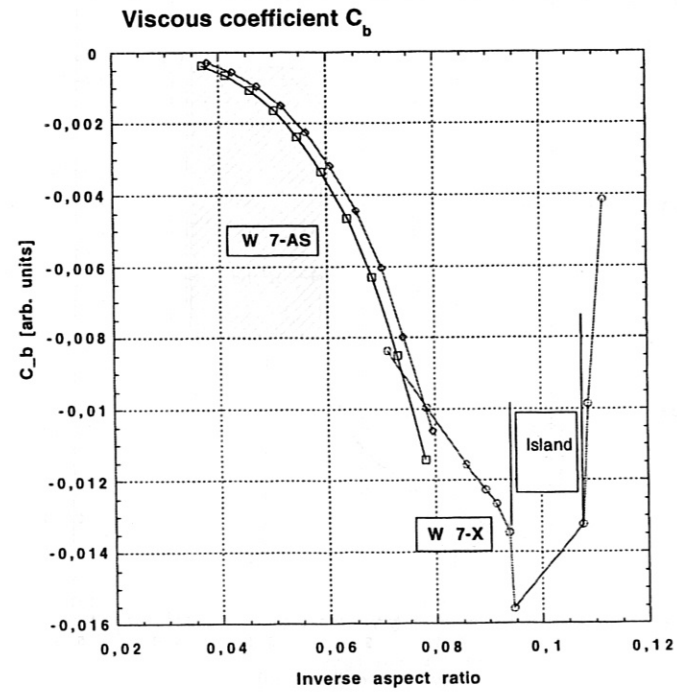

Fig. 22: Mixed coefficients in Wendelstein 7-AS and 7-X

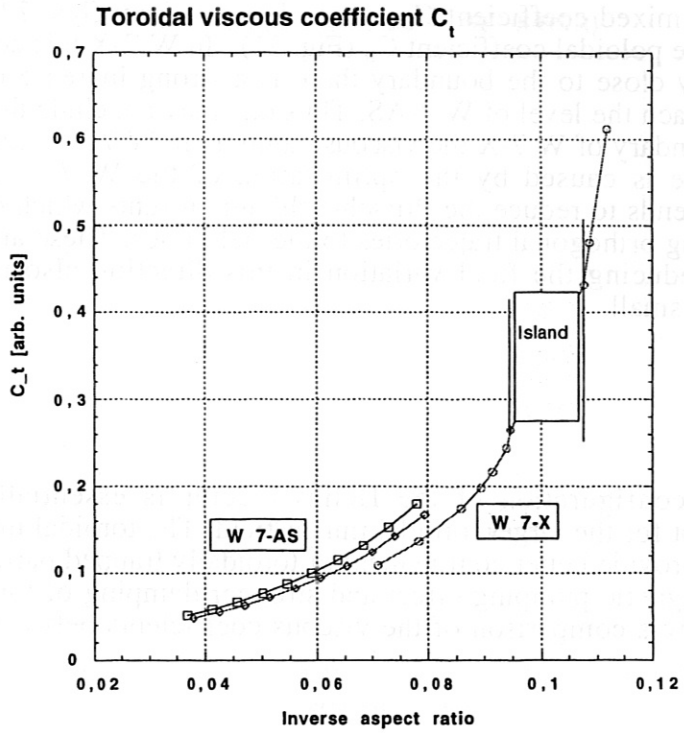

Fig. 23: Toroidal coefficients in Wendelstein 7-AS and 7-X

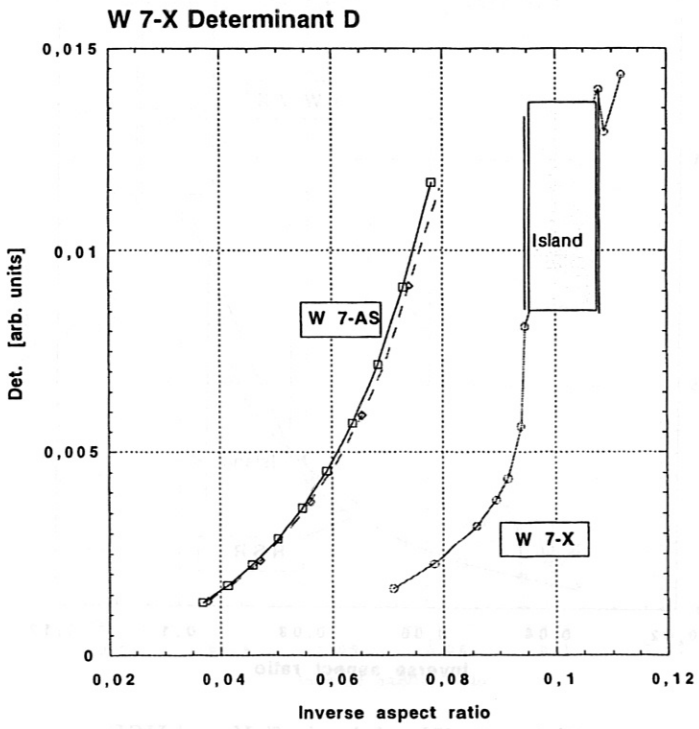

Fig. 24: Determinant of viscous coefficients.

There is nearly no difference between W 7-AS and W 7-X with respect to the toroidal coefficient C_t and the mixed coefficient C_b. as can be seen from figs. 22 and 23. The main difference occurs in the poloidal coefficient C_p (Fig. 21). In W 7-X this coefficient is smaller than in W 7-AS. Only close to the boundary there is a strong increase towards the island, however it does not reach the level of W 7-AS. Thus one may conclude that even in presence of 5 islands in the boundary of W 7-X the viscous damping in W 7-X is much smaller than in W 7-AS. This feature is caused by the optimisation of the W 7-X configuration. The optimisation scheme tends to reduce the Pfirsch-Schlüter currents which can be achieved by making ∇B small along orthogonal trajectories to the field lines. These are poloidally closed lines and therefore reducing the field variation in this direction also makes the poloidal viscous coefficient C_p small.

VI Helias Reactor

The magnetic field configuration of the Helias reactor is essentially the same as in Wendelstein 7-X exept for the larger toroidal mirror field. The toroidal mirror field has been increased in order to provide better confinement of toroidally trapped particles. This certainly will yield a larger magnetic pumping effect and stronger damping of toroidal rotation. The following figures show a comparison of the viscous coefficients between Wendelstein 7-X and the Helias reactor.

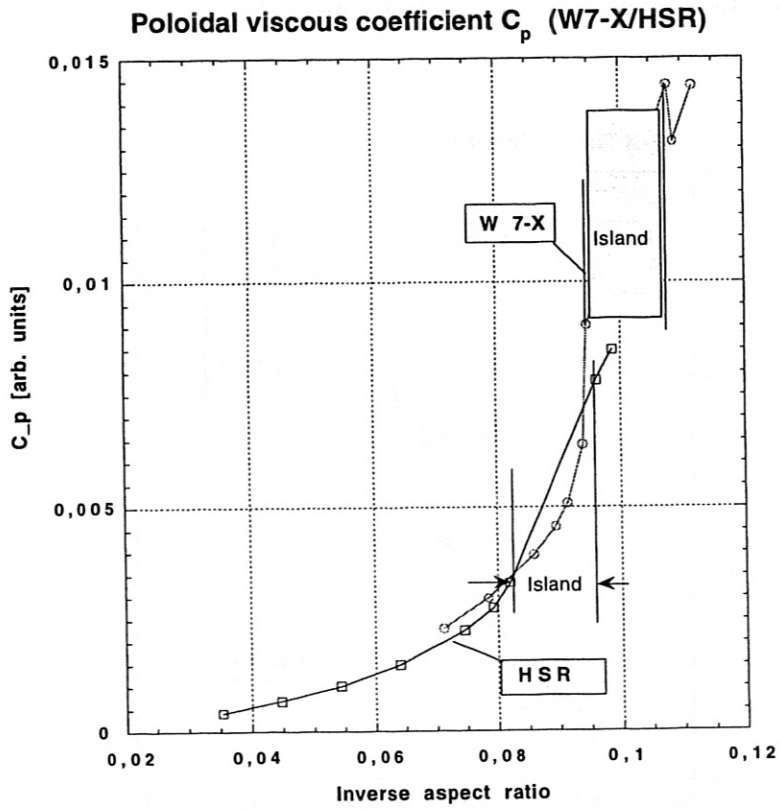

Fig. 25 : Poloidal viscous coefficient in Wendelstein 7-X and HSR

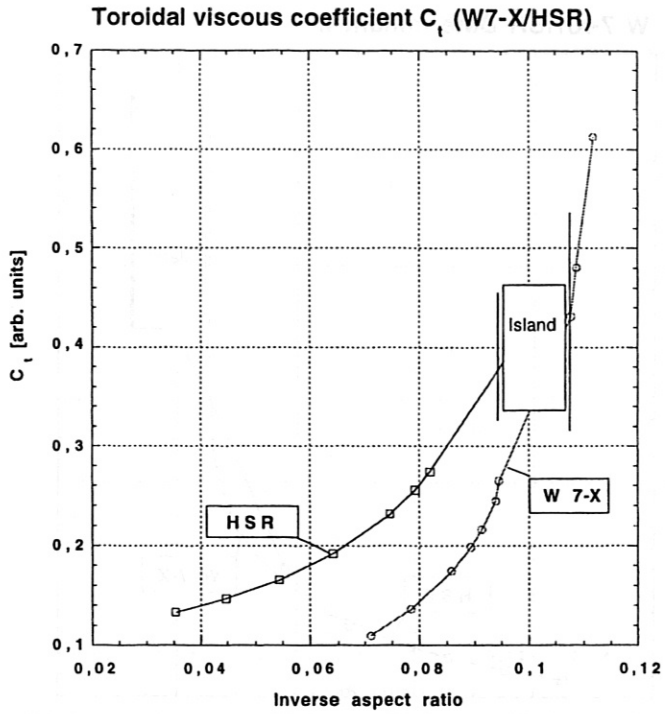

Fig. 26 : Toroidal viscous coefficient in Wendelstein 7-X and HSR

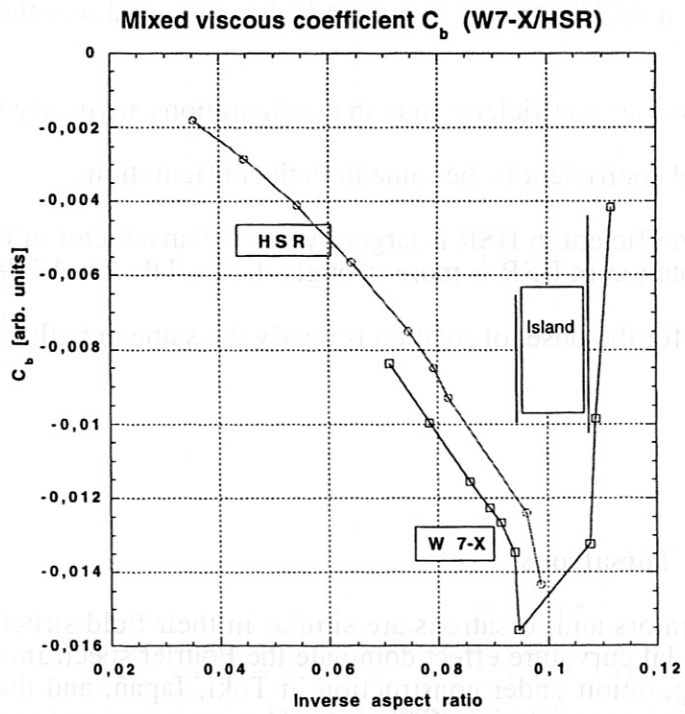

Fig. 27 : Mixed viscous coefficient in Wendelstein 7-X and HSR

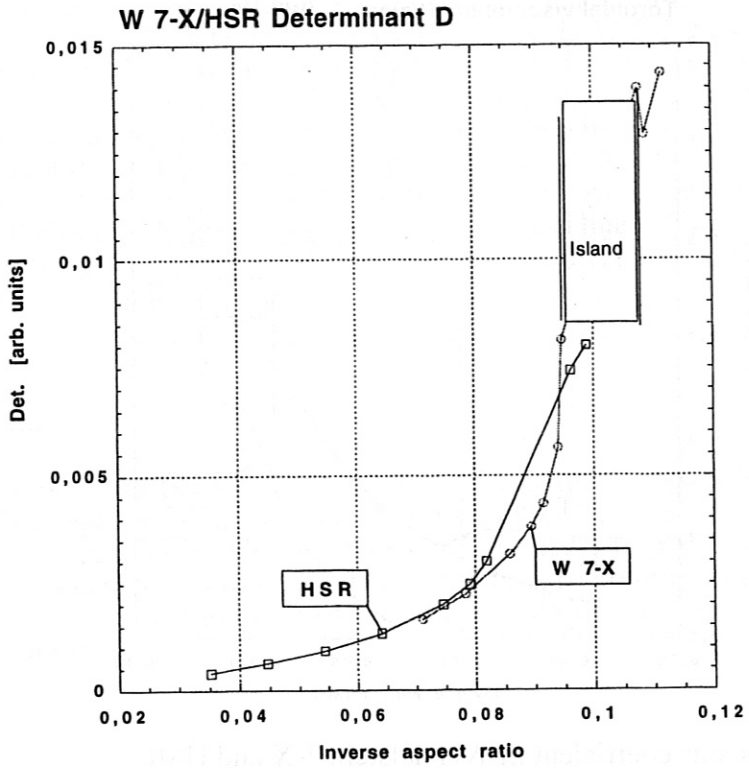

Fig. 28: Determinant (threshold) in W 7-X and HSR

The comparison between Wendelstein 7-X and the Helias reactor shows the following features:

-The poloidal viscous coefficients in both configurations are nearly the same (Fig. 25)

- Also the mixed coefficient is the same in both configurations

- The toroidal coefficient in HSR is larger by more than a factor of two, this implies that toroidal rotation in HSR is more strongly damped than in W 7-X

- The threshold for the onset of rotation is nearly the same in both cases (Fig. 28)

VII Comparison with Torsatrons

Standard l=2 stellarators and torsatrons are similar in their field structure, a large helical harmonic and the toroidal curvature effect dominate the Fourier spectrum of B. LHD is a 10-period torsatron configuration under construction in Toki, Japan, and the following figures show the viscous coefficients of this configuration. The inverse aspect ratio is larger in LHD than in W 7-X and the rotational transform ranges from 0.3 to 1.15. In the following computations islands in the boundary region of LHD are not taken into account.

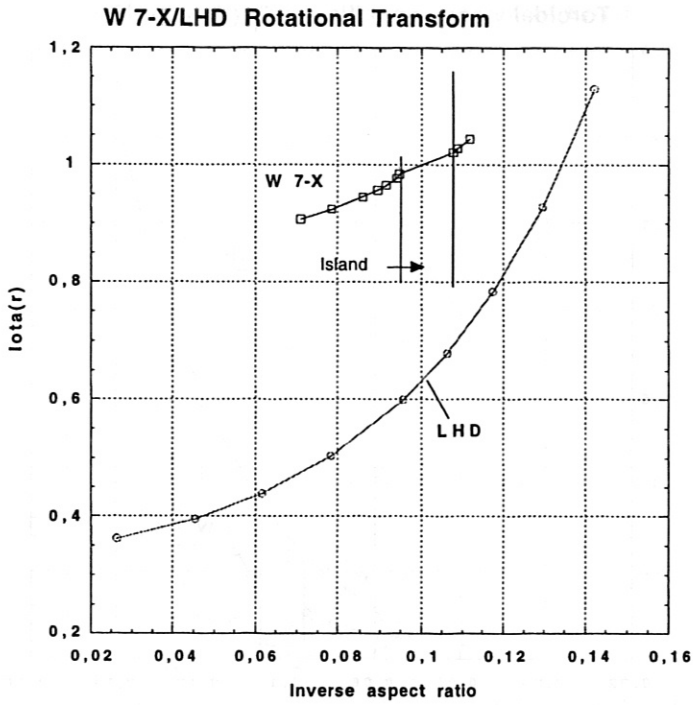

Fig. 30: Rotational transform vs inverse aspect ratio (W 7-X and LHD)

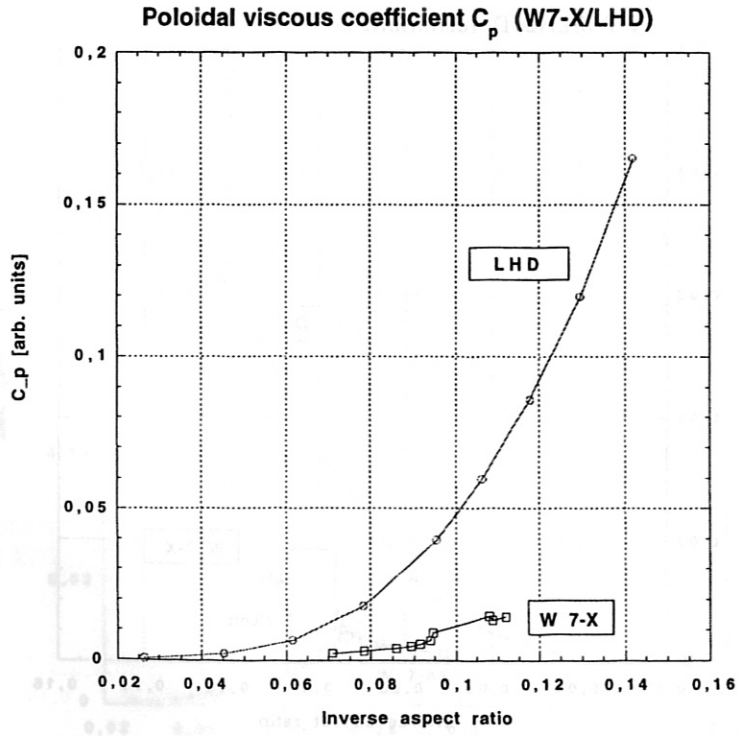

Fig. 31 Poloidal viscous coefficient of LHD and W 7-X

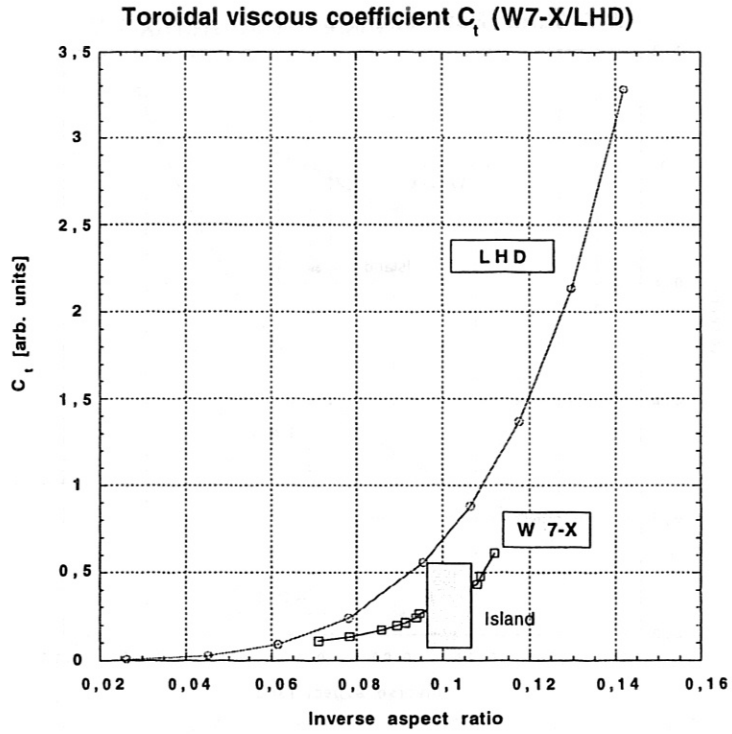

Fig. 32 Toroidal viscous coefficient of LHD and W 7-X

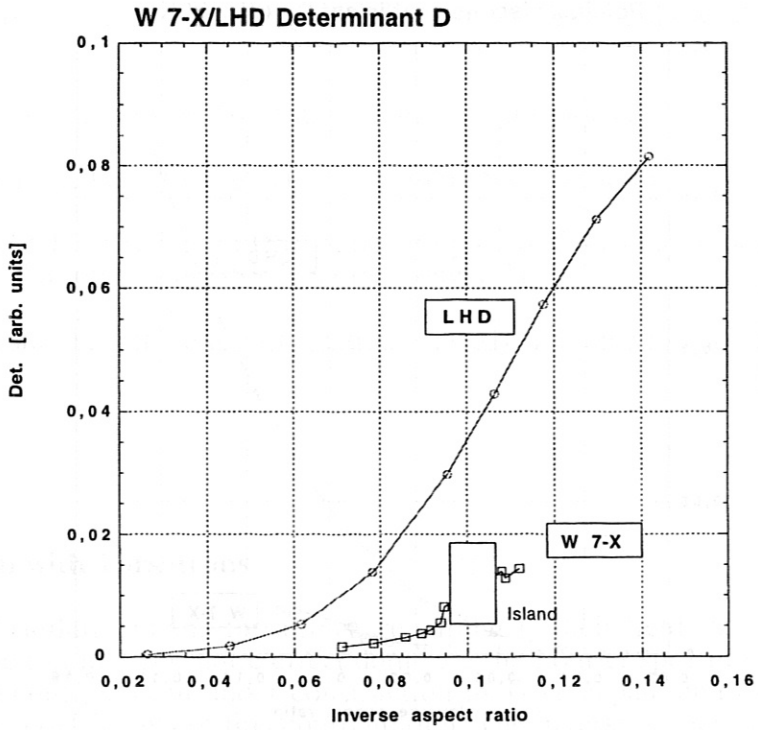

Fig. 33: Threshold of plasma rotation

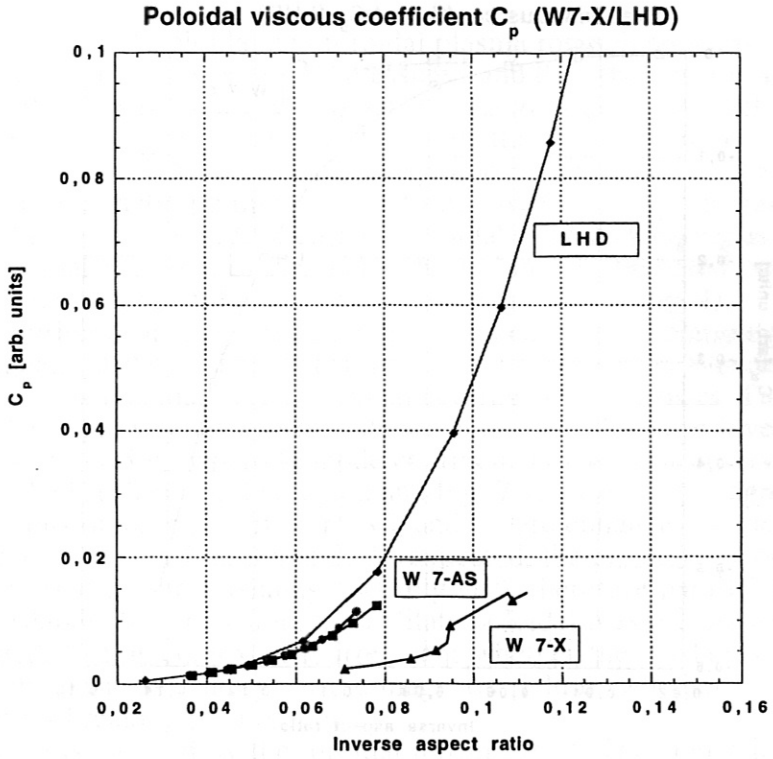

Fig. 34: Poloidal viscous coefficient (Wendelstein 7-AS, Wendelstein 7-X, LHD)

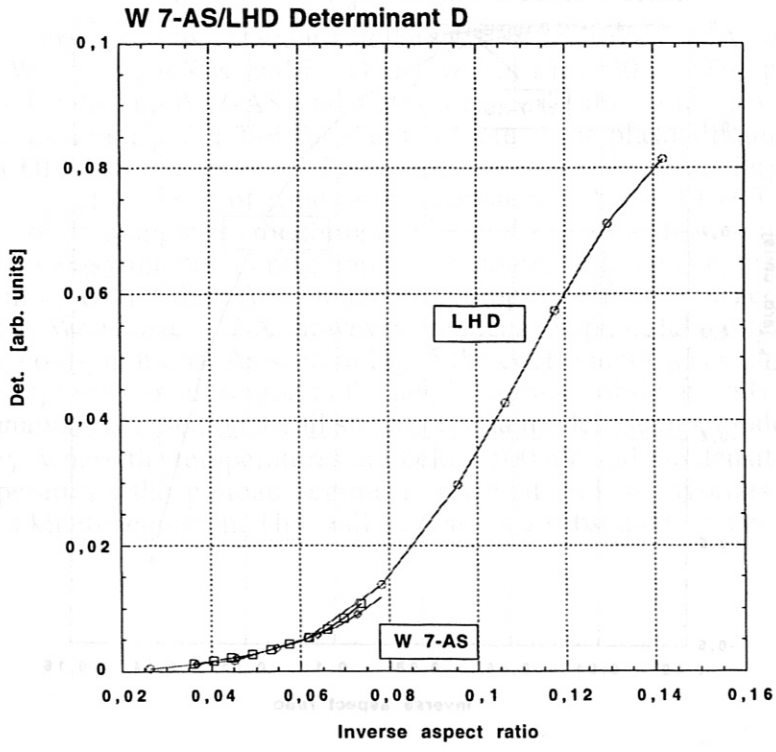

Fig. 35: Threshold of plasma rotation. Comparison W 7-AS - LHD.

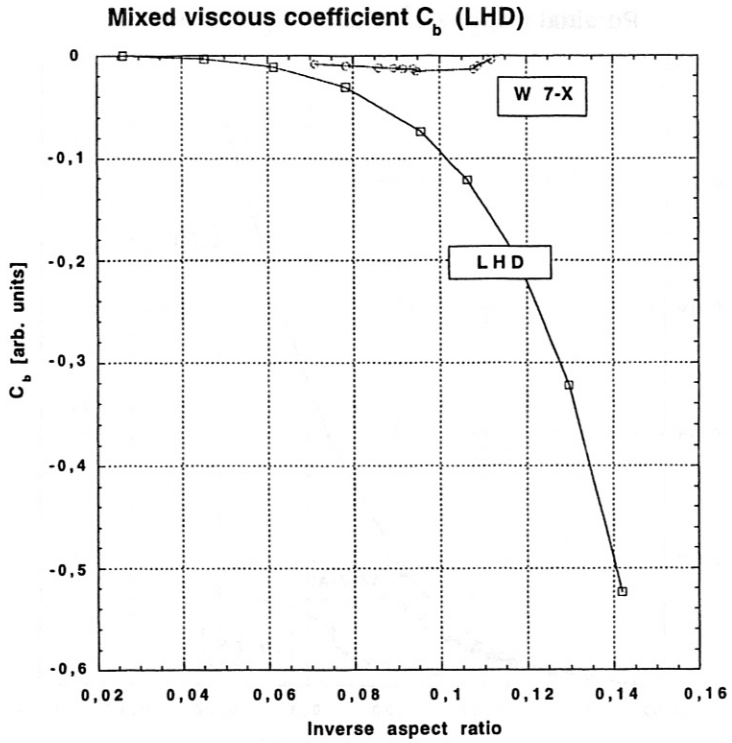

Fig. 36: Mixed coefficient C_b of W 7-X and LHD

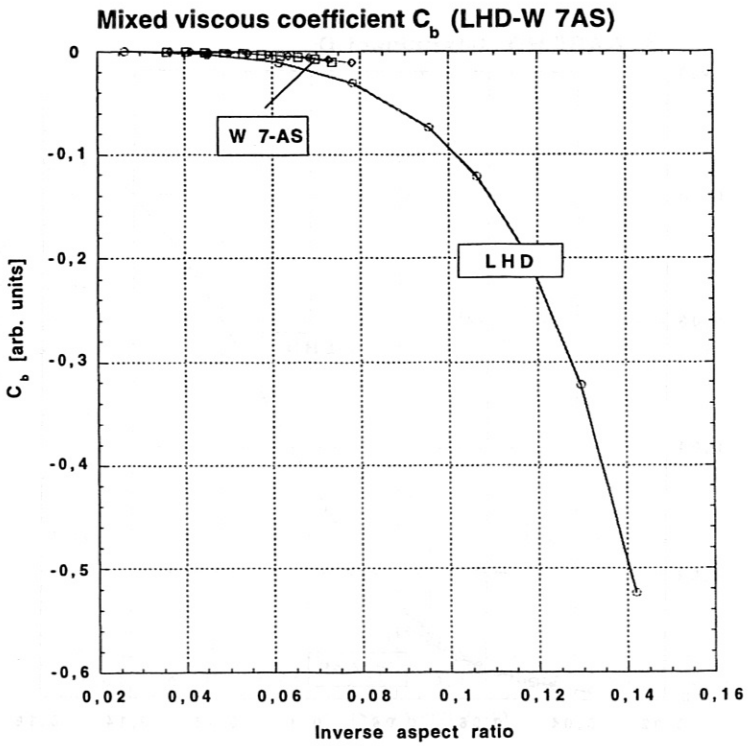

Fig. 37: Mixed coefficient C_b of W 7-AS and LHD

VIII Discussion

The viscous damping of poloidal and toroidal plasma rotation depends on two factors, one factor is τP - collision time times plasma pressure - and the other term is a geometrical factor C_p, C_t and C_b. With respect to the geometrical factor significant differences among the various stellarators exist, as has been shown in the figures above. C_p is the relevant geometrical factor of poloidal rotation. In axisymmetric devices only the toroidal curvature effect gives rise to magnetic pumping and a finite coefficient C_p. In stellarators, however, additional helical harmonics lead to increased poloidal viscous damping as is shown in Fig. 4. Reducing the poloidal variation of B - as has been done in optimised configurations of the Helias type - also reduces the poloidal viscous damping (Fig. 3, Fig. 4).

In the neighbourhood of magnetic islands enhanced viscous damping arises due to the distortion of magnetic surfaces. This effect may be of importance in Wendelstein 7-AS, where magnetic islands in the boundary region strongly corrugate the surfaces. The Fourier spectrum of B is modified and the viscous coefficients are enhanced. We have investigated the region between $\iota = 0.5$ and $\iota = 5/9$, where H-mode confinement has been observed in W 7-AS. Fig 6. shows unperturbed surfaces in this region and Fig. 7 surfaces with magnetic islands around $\iota = 5/9$. The viscous damping coefficients C_p and C_b are enhanced in the neighbourhood of the islands as can be seen in Fig. 8 and 9. As expected, the parallel viscous coefficient C_t is only slightly modified by these islands (see Fig. 10), therefore parallel plasma flow is not impeded by the islands. In conclusion, to facilitate poloidal plasma rotation magnetic islands should be avoided. In this context it is irrelevant whether these islands are natural islands which preserve the basic symmetry of the magnetic field or whether islands are caused by external symmetry - breaking perturbations.

Toroidal rotation is damped by the toroidal mirror effect. The coefficient C_t, which is the relevant coefficient of toroidal rotation, is nearly the same in Wendelstein 7-AS and Wendelstein 7-X (see Fig. 23). However, the Helias reactor exhibits a stronger toroidal damping due to the large toroidal mirror field (Fig. 26). This does not affect the threshold of plasma rotation since this number is mainly determined by the poloidal coefficient C_p (Fig. 28).

Torsatrons are very much like standard stellarators of the l=2-type. A comparison of Wendelstein 7-AS , Wendelstein 7-X and LHD is given in Figs. 30 ff. The poloidal coefficient and the threshold value in W 7-AS and LHD are nearly the same (see Figs. 34 and 35). Because of the different aspect ratios the damping rate at the plasma boundary increases to a larger value in LHD than it does in W 7-AS. The mixed coefficient is larger in LHD than in W 7-AS. With respect to onset of rotation Wendelstein 7-AS and LHD are equivalent - at least on the basis of damping rates. Nothing can be said about the driving mechanism.

In comparison to axisymmetric configurations standard stellarators exhibit a more complex Fourier spectrum of B and therefore magnetic pumping effect is larger. The optimisation scheme realised in Wendelstein 7-X, however, reduces the poloidal damping rate to the level of axisymmetric configurations. As seen in Fig. 5 the coefficient C_p is nearly the same in both configurations exept for a small region in the neighbourhood of the islands.

The present analysis is based on a collisional plasma model. Such a model is applicable to a plasma boundary, where the temperatures are below 100 eV and the densities above 10^{19} m^{-3}. At higher temperatures the plateau regime is reached and the viscous damping must be computed from a kinetic equation. This will be done in a subsequent paper.